Equalization and Performance of Diffusive Molecular Communication Systems with Binary Molecular-Shift Keying Modulation

Lu Shi, *Student Member, IEEE* and Lie-Liang Yang, *Fellow, IEEE*

***Abstract*—This paper investigates the equalization techniques for the diffusive molecular communication (DMC) systems with binary molecular-shift keying (BMoSK) modulation, referred to as the BMoSK-DMC systems, in order to mitigate the effect of inter-symbol interference (ISI). We first show that in terms of receiving equalization, a BMoSK-DMC system is in fact equivalent to a conventional binary phase-shift keying (BPSK) modulated radio communication system encountering ISI. Hence, a wealth of equalization techniques developed with the conventional radio communication systems may be introduced for equalization of BMoSK-DMC signals. However, considering the limited capability of molecular transceivers on computation and storage, in this paper, we investigate only the linear equalizers (LEQ) in the principles of matched-filtering (MF), zero-forcing (ZF) and minimum mean-square error (MMSE). We characterize the effects of the different aspects related to DMC signalling and propagation on the achievable performance of the BMoSK-DMC systems with these linear equalizers. Our studies and performance results demonstrate that both the ZF- and MMSE-LEQ are capable of efficiently suppressing the ISI and attaining promising performance, while still have low-complexity to facilitate implementation.**

I. Introduction

Design of the communication schemes operable at nano-scale has been motivated by researchers in order to implement intelligent drug delivery, neuroscience, network of nano-robots, and many other potential applications, as evidenced by the references [1–15] and the references therein. Inspired by nature, diffusive molecular communications (DMC) has become an emerging nano-scale communication paradigm, where information may be conveyed by encoding it into the value of molecular concentration, molecular type and release time at the transmitter [1]. During signal transmission, molecules can be driven by the Brownian motion with or without drift from the communication medium [16–18]. Hence, DMC can be a highly energy efficient communication scheme operable at nano-scale.

DMC has been investigated from different perspectives, as shown, for example, by the survey and tutorial paper [1] and the references therein. Specifically in the context of the DMC channel modelling, various channel and noise models have been proposed [16, 17]. It is shown that due to the random diffusive movements of molecules, DMC usually experiences strong inter-symbol interference (ISI), in addition to the noise generated from the random movements of information molecules as well as from the other possible noisy sources in the environment [17]. In literature, various ISI mitigation techniques have been proposed and investigated. These techniques can in general be classified into the transmitter signalling design and the receiver signal processing. In a little more detail, in the class of the transmitter signalling design, the molecular shift keying (MoSK) modulation scheme [19, 20] has the embedded capability of ISI mitigation, as multiple types of molecules are used for information encoding, resulting in that the same type of molecules has a relatively small probability to become active. Relying on two types of molecules, the molecular transition shift keying (MTSK) modulation [21] has been proposed specifically for ISI mitigation. With the MTSK, no molecules are emitted for transmitting bit 0, while a type of molecules is released for transmitting a bit 1 followed by a bit 1, and the second type of molecules is emitted for transmitting a bit 1 followed by a bit 0. Furthermore, a modulation scheme based on multiple types of molecules has been proposed in [22]. With this transmission scheme, the same type of molecules is only allowed to be activated after a pre-defined time period.

In the context of the receiver signal processing techniques for ISI mitigation/suppression. One way is to use the interference suppression/cancellation [23–29], which first generates an estimate to the ISI and then subtracts the estimated ISI from the observation for information detection. Another approach is to use the equalization techniques. In literature, various equalization methods have been proposed, as shown, e.g., in [25, 30–32]. In more detail, these equalization techniques include the sequence detectors in the principles of maximum a-posteriori (MAP) or maximum likelihood (ML) [25, 30–33], linear equalizer in minimum mean-square error (MMSE) principle [31] or in zero-forcing (ZF) principle [34, 35], the decision-feedback based equalization [31, 36], etc. In all these references considering the equalization techniques, concentration-shift keying (CSK) modulation has been considered.

Following the research in literature, in this paper, we consider the equalization in the binary molecular shift keying DMC (BMoSK-DMC) systems. We assume that in the BMoSK-DMC system, two types of molecules having the same propagation property are used for binary data modulation, where one type is activated to transmit bit 1, while the other type is activated to transmit bit 0. At the receiver, the differences between the sampled concentrations of the two

L. Shi and L.-L. Yang are with School of Electronics and Computer Science, University of Southampton, SO17 1BJ, UK. (E-mail: ls25g12, lly@ecs.soton.ac.uk, https://www.ecs.soton.ac.uk/people/llyang).

types of molecules are used as the observations for information detection. We demonstrate that the differences between the sampled concentrations of the two types of molecules have an equivalent structure as the observations in the conventional radio-based communication systems with binary phase-shift keying (BPSK) modulation and experiencing ISI [37]. Therefore in theory, various equalization techniques introduced to the conventional radio-based communications can be employed to equalize the DMC channel and improve the detection reliability of the BMoSK-DMC system. However, we should be aware of that at nano-scale, the transceivers deployed with DMC usually have limited signal processing capability, and hence the non-linear high-complexity equalization techniques based on, e.g., MAP or ML, may be impractical. Therefore, in this paper, we investigate and compare the performance of the BMoSK-DMC systems with only the linear equalization (LEQ) based on the matched-filtering (MF), zero-forcing (ZF) and minimum mean-square error (MMSE) principles, referred to as the MF-LEQ, ZF-LEQ and MMSE-LEQ, respectively.

In summary, the main contributions and novelties of the paper are as follows.

- Signal detection and equalization are investigated in the context of the BMoSK-DMC system, in contrast to the references where equalization has been mainly investigated with the CSK modulation.
- An expression is derived for representing the received signals in the BMoSK-DMC system, which has the same form as the received signals in the conventional radio-based BPSK-modulated communication systems experiencing ISI. Hence, it enables the feasibility to be empowered by the equalization techniques developed with the conventional radio-based communications.
- Hence, the MF-LEQ, ZF-LEQ and MMSE-LEQ are introduced to the BMoSK-DMC system.
- Furthermore, the performance of the BMoSK-DMC system with MF-LEQ, ZF-LEQ and MMSE-LEQ is investigated and compared based on numerical simulations.

In the rest of paper, the system model is first introduced in Section II. Section III provides the expressions for the received signals, which are beneficial to the derivation of equalizers. In Section IV, we detail the equalization schemes. Performance results are demonstrated in Section V. Finally in Section VI, we conclude the paper with a summary of the research.

II. System Model

The BMoSK-DMC system to be considered consists of a point-source transmitter and a point-like receiver. The locations of transmitter and receiver are separated by a distance r, as shown in Fig. 1. Information is transmitted by releasing a pulse of Q number of molecules at the beginning of each fixed bit duration T_b. We assume that the receiver is capable of counting the number of information molecules inside a spherical detection space with a radius of ρ, and hence a volume of $V = 4\pi\rho^3/3$. The transmitter uses BMoSK modulation to send binary information data $\{b_j\} = \{b_0, b_1, \dots, b_j, \dots\}$, where $b_j \in \{0, 1\}$, with the aid of two types of molecules, recorded as Type-A and Type-B. Type-A is assigned for signalling $b_j = 1$ and Type-B is for signalling $b_j = 0$. We assume that the number Q of molecules emitted per pulse obeys the Poisson distribution with a rate λ within a sufficiently short time. Furthermore, we assume that the fluid medium is stable with a constant diffusion coefficient D. Additionally, we assume that synchronization is achieved between transmitter and receiver.

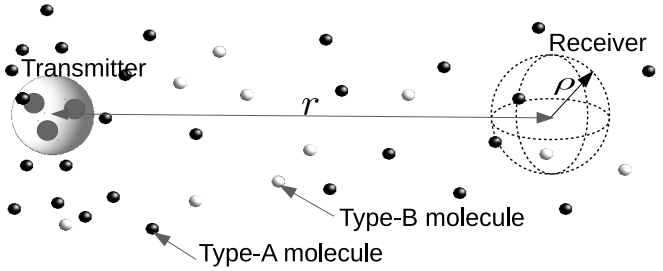

Fig. 1. System model for DMC systems with BMoSK modulation, where the dark and light coloured small spheres represent the Type-A and Type-B molecules.

Based on the above assumptions and assuming that a pulse of Q molecules is emitted by the transmitter at $t = 0$, the concentration measured by the receiver at time $t > 0$ follows the Fick's Law, and is expressed as

$$c(t) = \frac{Q}{(4\pi Dt)^{\frac{3}{2}}} \exp\left(-\frac{r^2}{4Dt}\right), t > 0, \tag{1}$$

which is a time-domain pulse function when observed at the receiver, and reaches its maximum at the time $t_d = r^2/6D$. By substituting this value into Eq. (1), its peak concentration value is given by $c_{\max} = \left(\frac{3}{2\pi e}\right)^{\frac{3}{2}} \frac{Q}{r^3}$, which decreases shapely with the increase of transmission distance. For this sake and when there is no drift, DMC is usually only suitable for the communications over short distance.

When assuming that the receiver is capable of identifying the two types of molecules, the concentration difference between Type-A and Type-B molecules sensed by the receiver for the uth bit can be expressed as

$$\begin{aligned} z(t) =& z_A(t) - z_B(t) \\ =& \sum_{j=0}^{u} b_j [c_A(t - jT_b) + n_{A,j}(t)] \\ & - \sum_{j=0}^{u} (1 - b_j)[c_B(t - jT_b) + n_{B,j}(t)], \\ & uT_b \le t < (u+1)T_b, \end{aligned} \tag{2}$$

where $c_X(t - jT_b)$, $X \in \{A, B\}$, is the concentration sensed at time t, $uT_b \le t < (u+1)T_b$, generated by the molecular pulse for sending the jth bit b_j sent during $jT_b \le t < (j+1)T_b$. This is the interference of the jth transmitted bit on the receiving of the uth bit. Hence, BMoSK-DMC experiences inter-symbol interference (ISI), which can be very severe, and significantly degrades the communication reliability, especially, when the transmission rate is relatively high, or when the transmission distance is relatively long. In Eq. (2), $n_{A,j}(t)$ and $n_{B,i}(t)$ are the particle counting noise caused by the corresponding types of molecules emitted by

the jth pulse of molecules [17]. Considering one particular type of molecules, since the number of emitted molecules per pulse is assumed to obey the Poisson distribution with a rate λ, we can readily know that $V[c_A(t-jT_b)+n_{A,j}(t)]$ (or $V[c_B(t-jT_b)+n_{B,j}(t)]$) obeys the Poisson distribution with the rate $\lambda V c_A(t-jT_b)$ (or $Vc_B(t-jT_b)$). Hence, according to [17, 25], when Q in Eq. (1) is sufficiently large, $n_{A,j}(t)$ (or $n_{B,j}(t)$) can be approximated as the Gaussian noise with zero mean and a variance of $\sigma^2_{A,j}(t) = V^{-1}b_j c_A(t-jT_b)$ (or $\sigma^2_{B,j}(t) = V^{-1}(1-b_j)c_B(t-jT_b)$), when $b_j = 1$ (or $b_j = 0$) is transmitted. For convenience, these normal distributions can be expressed as $n_{A,j}(t) \sim \mathcal{N}\left(0, \sigma^2_{A,j}(t)\right)$ or $n_{B,j}(t) \sim \mathcal{N}\left(0, \sigma^2_{B,j}(t)\right)$.

In order to detect the uth bit, the receiver samples for the concentrations at $t = uT_b + \hat{t}_d$, where $\hat{t}_d$ is the estimated t_d. Then, the concentration difference between Type-A and Type-B molecules at the sampling time $t = uT_b + \hat{t}_d$ can be expressed as

$$\begin{aligned} z_u =& z_A(t = uT_b + \hat{t}_d) - z_B(t = uT_b + \hat{t}_d) \\ =& \sum_{j=0}^{u} b_j[c_A((u-j)T_b + \hat{t}_d) + n_{A,j,u}] \\ & - \sum_{j=0}^{u}(1-b_j)[c_B((u-j)T_b + \hat{t}_d) + n_{B,j,u}], \\ & u = 0, 1, \ldots, \end{aligned} \tag{3}$$

where $n_{A,j,u} = n_{A,j}(uT_b + \hat{t}_d)$ and $n_{B,j,u} = n_{B,j}(uT_b + \hat{t}_d)$, which are the noise added on the uth bit but due to the transmission of the jth bit. Explicitly, the detection of bit u experiences the ISI imposed from the bits sent in the front of bit u, i.e., via the indices of $j = 0, 1, \ldots, u-1$, as seen in Eq. (3). Let us assume that the maximum length of ISI is L bits. The value of L can be derived by letting the ISI to be ignorable in relative to the desired signal, as done, for example, in [24]. Then, z_u in Eq. (3) can be expressed in the form of

$$\begin{aligned} z_u =& \sum_{j=\max\{0,u-L\}}^{u} b_j[c_A((u-j)T_b + \hat{t}_d) + n_{A,j,u}] \\ & - \sum_{j=\max\{0,u-L\}}^{u} (1-b_j)[c_B((u-j)T_b + \hat{t}_d) + n_{B,j,u}], \\ & u = 0, 1, \ldots. \end{aligned} \tag{4}$$

Let $i = u - j$, $c_{A,i} = c_A(iT_b + \hat{t}_d)$ and $c_{B,i} = c_B(iT_b + \hat{t}_d)$, we can re-represent Eq.Eq. (4) as

$$\begin{aligned} z_u =& \sum_{i=0}^{\min\{u,L\}} [b_{u-i}c_{A,i} - (1-b_{u-i})c_{B,i}] \\ & + \sum_{i=0}^{\min\{u,L\}} [b_{u-i}n_{A,u-i,u} - (1-b_{u-i})n_{B,u-i,u}], \\ & u = 0, 1, \ldots, \end{aligned} \tag{5}$$

where, again, $n_{A,u-i,u}$ and $n_{B,u-i,u}$ are the Type-A and Type-B noise imposing on the uth bit, but generated by the transmission of the $(u-i)$th bit. It can be shown that $n_{A,u-i,u}$ and $n_{B,u-i,u}$ obey the distributions of $n_{A,u-i,u} \sim \mathcal{N}\left(0, \sigma^2_{A,u-i,u}\right)$ or $n_{B,u-i,u} \sim \mathcal{N}\left(0, \sigma^2_{B,u-i,u}\right)$, where $\sigma^2_{A,u-i,u} = V^{-1}c_{A,i}$ and $\sigma^2_{B,u-i,u} = V^{-1}c_{B,i}$.

III. Representation of Received Molecular Signals

Despite that the types of molecules for Type-A and Type-B are different, as implied from Eq. (1), we have $c_{A,i} = c_{B,i} = c_i$, when the number Q of molecules per transmission pulse, and the medium diffusion coefficient D are the same. Furthermore, let $n_{u-i} = b_{u-i}n_{A,u-i,u} - (1-b_{u-i})n_{B,u-i,u}$. Then, we can readily show that n_{u-i} has the distribution of $n_{u-i} \sim \mathcal{N}\left(0, \sigma^2_{u-i}\right)$ with $\sigma^2_{u-i} = V^{-1}c_i$, when the Gaussian approximation is applied. When applying these results into Eq. (5), we can obtain z_u as

$$\begin{aligned} z_u =& \sum_{i=0}^{\min\{u,L\}} \left(2b_{u-i} - 1\right)c_i \\ & + \sum_{i=0}^{\min\{u,L\}} n_{u-i}, \ u = 0, 1, \ldots. \end{aligned} \tag{6}$$

Here we should note that, although the Gaussian approximation of n_{u-i} may not be accurate, the Gaussian approximation of $\sum_{i=0}^{\min\{u,L\}} n_{u-i}$ can usually be sufficiently accurate for studying the performance of DMC systems, as demonstrated in [24]. In order to facilitate the mathematical derivation, let in Eq. (6) $\tilde{b}_{u-i} = 2b_{u-i} - 1$, where we now have $\tilde{b}_{u-i} \in \{-1, 1\}$, and $n_u = \sum_{i=0}^{\min\{u,L\}} n_{u-i}$, which follows the distribution of $n_u \sim \mathcal{N}\left(0, \sigma^2_n = V^{-1}\sum_{i=0}^{\min\{u,L\}} c_i\right)$. Then, we can modify Eq. (6) to

$$z_u = \sum_{i=0}^{\min\{u,L\}} \tilde{b}_{u-i}c_i + n_u, \ u = 0, 1, \ldots. \tag{7}$$

Let us assume that the system is operated in its static state, meaning that $u >> L$. Also, let us assume that there is a $(N+L)$-length bit sequence expressed as $\boldsymbol{b} = [b_{-L}, \ldots, b_{-1}, b_0, b_1, \ldots, b_{N-1}]^T$, where $b_{-L}, \ldots, b_{-1}$ are the L bits sent in the front of b_0. Corresponding to $\boldsymbol{b}$, we have $\tilde{\boldsymbol{b}}$, whose elements have values in $\{+1, -1\}$. Let the signals received in correspondence to $[b_0, b_1, \ldots, b_{N-1}]^T$ be expressed as $\boldsymbol{y} = [z_0, z_1, \ldots, z_{N-1}]^T$, the corresponding noise samples be expressed as $\boldsymbol{n} = [n_0, n_1, \ldots, n_{N-1}]^T$. Then, the received signals $\boldsymbol{y}$ can be expressed in matrix form as

$$\boldsymbol{y} = \boldsymbol{H}\tilde{\boldsymbol{b}} + \boldsymbol{n}, \tag{8}$$

where $\boldsymbol{H}$ is the $N \times (N+L)$ dimensional matrix due to channel impulse responses. The (i,j)th element of $\boldsymbol{H}$ is given by

$$h_{i,j} = \begin{cases} c_{i-j+L}, & \text{when } -L \le i-j \le 0 \\ 0, & \text{otherwise} \end{cases}, \tag{9}$$
$$i = 0, 1, \ldots, N-1; j = 0, 1, \ldots, N+L-1.$$

In more detail, $\boldsymbol{H}$ is in the form of

$$\boldsymbol{H} = \begin{pmatrix} c_L & \cdots & c_1 & c_0 & 0 & \cdots & \cdots & \cdots & \cdots & 0 \\ 0 & c_L & \cdots & c1 & c_0 & 0 & \cdots & \cdots & \cdots & 0 \\ \vdots & \ddots & \ddots & \ddots & \ddots & \ddots & \ddots & \ddots & \ddots & \vdots \\ 0 & \cdots & \cdots & \cdots & \cdots & \cdots & c_L & \cdots & c_1 & c_0 \end{pmatrix}. \tag{10}$$

In Eq. (8), $\boldsymbol{n}$ is a Gaussian noise vector, which has zero mean and a covariance matrix of $\sigma_n^2 \boldsymbol{I}_N$, with $\sigma_n^2 = V^{-1} \sum_{i=0}^{L} c_i$ and $\boldsymbol{I}_N$ being the identity matrix of size $(N \times N)$.

Furthermore, if we express $\tilde{\boldsymbol{b}} = [\tilde{\boldsymbol{b}}_I^T, \tilde{\boldsymbol{b}}_d^T]^T$, where $\tilde{\boldsymbol{b}}_I = [\tilde{b}_{-L}, \tilde{b}_{-L+1}, \ldots, \tilde{b}_{-1}]^T$, and $\tilde{\boldsymbol{b}}_d = [\tilde{b}_0, \tilde{b}_1, \ldots, \tilde{b}_{N-1}]^T$. Again, corresponding to $\tilde{\boldsymbol{b}}_I$ and $\tilde{\boldsymbol{b}}_d$, we have their one-to-one mappings to $\boldsymbol{b}_I$ and $\boldsymbol{b}_d$. Corresponding to $\tilde{\boldsymbol{b}}_I$ and $\tilde{\boldsymbol{b}}_d$, let us divide $\boldsymbol{H}$ into $\boldsymbol{H}_I$ and $\boldsymbol{H}_d$, which consist of the first L columns and the other N columns of $\boldsymbol{H}$, respectively. Then, we can rewrite Eq. (8) as

$$\boldsymbol{y} = \boldsymbol{H}_d \tilde{\boldsymbol{b}}_d + \boldsymbol{H}_I \tilde{\boldsymbol{b}}_I + \boldsymbol{n}. \tag{11}$$

From this representation, explicitly, $\boldsymbol{H}_I \tilde{\boldsymbol{b}}_I$ is the interference imposed by the last data block on the current data block $\tilde{\boldsymbol{b}}_d$.

IV. Equalization Algorithms

In this section, we consider some equalization schemes for detecting the received information in the BMoSK-DMC system. Since nano-machines are usually tiny size with very limited power for computation, we consider only low-complexity linear equalization schemes. Specifically, we consider the equalization schemes in the principles of matched-filtering (MF), zero-forcing (ZF) and minimum mean-square error (MMSE). For all these three equalization schemes, the decision variables for detecting $\tilde{\boldsymbol{b}}_d$, and hence $\boldsymbol{b}_d$, can be obtained from the linear processing

$$\tilde{\boldsymbol{z}} = \boldsymbol{G}\boldsymbol{y}, \tag{12}$$

where $\boldsymbol{G}$ is a $(N \times N)$ linear processing matrix for generating N decision variables, which are determined in the principles of MF, ZF and MMSE, as detailed below.

A. Matched-Filtering Linear Equalization

When substituting $\boldsymbol{y}$ from Eq. (11) into Eq. (12), we obtain

$$\tilde{\boldsymbol{z}} = \boldsymbol{G}\boldsymbol{H}_d \tilde{\boldsymbol{b}}_d + \boldsymbol{G}\boldsymbol{H}_I \tilde{\boldsymbol{b}}_I + \boldsymbol{G}\boldsymbol{n}, \tag{13}$$

which gives N decision variables for the N bits in $\tilde{\boldsymbol{b}}_d$.

In the context of the MF-assisted linear equalization (MF-LEQ), we choose $\boldsymbol{G}$ as [37]

$$\boldsymbol{G}_{MF} = \boldsymbol{H}_d^T. \tag{14}$$

Assume that $n > 2L$. In this case, the interference term $\boldsymbol{G}\boldsymbol{H}_I \tilde{\boldsymbol{b}}_I$ in Eq. (13) will not show in the decision variable for $\tilde{b}_n$. It can be shown that the last a few of decision variables for $\tilde{b}_n$ can be expressed as

$$\begin{aligned}
\tilde{z}_{N-1} =& c_0^2 \tilde{b}_{N-1} + \sum_{i=1}^{L} c_0 c_i \tilde{b}_{N-i-1} + n'_N, \\
\tilde{z}_{N-2} =& (c_0^2 + c_1^2)\tilde{b}_{N-2} + \sum_{i=1}^{L} c_0 c_i \tilde{b}_{N-2-i} \\
&+ \sum_{i=0, i\neq 1}^{L} c_1 c_i \tilde{b}_{N-1-i} + n'_{N-1}, \\
\tilde{z}_{N-3} =& (c_0^2 + c_1^2 + c_2^2)\tilde{b}_{N-3} + \sum_{i=1}^{L} c_0 c_i \tilde{b}_{N-3-i} \\
&+ \sum_{i=0, i\neq 1}^{L} c_1 c_i \tilde{b}_{N-2-i} + \sum_{i=0, i\neq 2}^{L} c_2 c_i \tilde{b}_{N-1-i} + n'_{N-1}, \\
\tilde{z}_{N-4} =& \left(\sum_{i=0}^{3} c_i^2 \right) \tilde{b}_{N-4} + \sum_{i=1}^{L} c_0 c_i \tilde{b}_{N-4-i} \\
&+ \sum_{i=0, i\neq 1}^{L} c_1 c_i \tilde{b}_{N-3-i} + \sum_{i=0, i\neq 2}^{L} c_2 c_i \tilde{b}_{N-2-i} \\
&+ \sum_{i=0, i\neq 3}^{L} c_2 c_i \tilde{b}_{N-1-i} + n'_{N-1}.
\end{aligned} \tag{15}$$

Similarly, we can write out the other decision variables. From the above equations we can know that, when the value of n decreases from $N-1$ to $N-L-1$, the decision variable $\tilde{z}_n$ is capable of collecting more power from the diffusive channels. However, the number of interference terms also increases. In Section V, we will investigate this issue to illustrate which of them is more dominant to the achievable performance.

The MF-LEQ has a low complexity for implementation. From Eq. (15) we can readily know that the complexity for detecting a bit is mainly contributed by the multiplication operations. Since the maximum number of non-zero elements in a column of $\boldsymbol{H}_d$ is $(L+1)$, the number of operations, including both multiplications and additions, is about $2L$. Hence, the complexity of the MF-LEQ is $\mathcal{O}(L)$ per bit. Furthermore, as above-mentioned, the best error performance should not be attained with $N-L-1$, but with a value close to $N-1$, as the result that the molecular density of Eq. (1) decreases sharply with the increase of time. As shown by our performance results in Section V, the best performance can usually be achieved for $N-1$ or $N-2$. In these cases, the number of operations required for detecting a bit is only about 2 or 4, which can be significantly lower than $\mathcal{O}(L)$.

B. Zero-Forcing Linear Equalization

Upon treating the inter-block interference $\boldsymbol{G}\boldsymbol{H}_I \tilde{\boldsymbol{b}}_I$ as Gaussian noise, the ZF linear equalizer (ZF-LEQ) can be directly obtained from Eq. (13) by the implementation of $\boldsymbol{G}\boldsymbol{H}_d = \boldsymbol{I}_N$. From Eq. (10) we can deduce that $\boldsymbol{H}_d$ is invertible, and its inverse is also a lower triangular matrix. Hence, we can readily obtain that

$$\boldsymbol{G}_{ZF} = \boldsymbol{H}_d^{-1}. \tag{16}$$

Upon substituting this result into Eq. (13), the decision variable vector $\tilde{\boldsymbol{z}}$ can be expressed as

$$\tilde{\boldsymbol{z}} = \tilde{\boldsymbol{b}}_d + \boldsymbol{H}_d^{-1}\boldsymbol{H}_I\tilde{\boldsymbol{b}}_I + \boldsymbol{H}_d^{-1}\boldsymbol{n}. \tag{17}$$

The ZF-LEQ has the following characteristics. First, it is capable of fully suppressing the ISI within $\tilde{\boldsymbol{b}}_d$. However, there is still some ISI from the bits sent in the front of $\tilde{b}_0$. Second, when given the transmission distance and sampling interval, $\boldsymbol{H}_d$ is a fixed matrix, and hence its inverse is also fixed and only required to be computed once. Therefore, the complexity of the ZF-LEQ is the same as that of the MF-LEQ. Finally, it is well known that ZF-LEQ has the problem of noise amplification [38]. However, from Eq. (13) we can know that $\boldsymbol{H}_d$ is a square matrix of diagonal elements significantly dominant, if the transmission distance is relatively short. Hence, we can expect that the N eigenvalues of $\boldsymbol{H}_d$ are all smaller but very close to one. Therefore, the noise amplification problem in the ZF-LEQ for DMC systems is usually not severe, as demonstrated in SectionV.

C. Minimum Mean-Square Error Linear Equalization

For the MMSE-LEQ, the optimum linear processing matrix $\boldsymbol{G}$ seen in Eq. (12) can be derived from the optimization problem expressed as

$$\boldsymbol{G}_{MMSE} = \arg\min_{\boldsymbol{G}} \mathbb{E}\left\{\|\tilde{\boldsymbol{b}}_d - \boldsymbol{G}\boldsymbol{y}\|^2\right\}. \tag{18}$$

Solving this optimization problem gives the MMSE-LEQ solution of [38]

$$\boldsymbol{G}_{MMSE} = \boldsymbol{R}_{\boldsymbol{y}\tilde{\boldsymbol{b}}_d}^T\boldsymbol{R}_{\boldsymbol{y}}^{-1}, \tag{19}$$

where $\boldsymbol{R}_{\boldsymbol{y}}$ is the autocorrelation matrix of $\boldsymbol{y}$, given by

$$\begin{aligned}\boldsymbol{R}_{\boldsymbol{y}} = \mathbb{E}\left\{\boldsymbol{y}\boldsymbol{y}^T\right\} &= \boldsymbol{H}\boldsymbol{H}^T + \sigma_n^2\boldsymbol{I}_N \\ &= \boldsymbol{H}_d\boldsymbol{H}_d^T + \boldsymbol{H}_I\boldsymbol{H}_I^T + \sigma_n^2\boldsymbol{I}_N,\end{aligned} \tag{20}$$

and $\boldsymbol{R}_{\boldsymbol{y}\tilde{\boldsymbol{b}}_d}$ is the cross-correlation matrix between $\boldsymbol{y}$ and $\tilde{\boldsymbol{b}}_d$, given by

$$\boldsymbol{R}_{\boldsymbol{y}\tilde{\boldsymbol{b}}_d} = \mathbb{E}\left\{\boldsymbol{y}\tilde{\boldsymbol{b}}_d^T\right\} = \boldsymbol{H}_d. \tag{21}$$

Substituting Eq. (20) and Eq. (21) into Eq. (19), we obtain $\boldsymbol{G}_{MMSE}$ as

$$\boldsymbol{G}_{MMSE} = \boldsymbol{H}^T\left(\boldsymbol{H}\boldsymbol{H}^T + \sigma_n^2\boldsymbol{I}\right)^{-1}. \tag{22}$$

The MMSE-LEQ employs the similar properties as the ZF-LEQ. It is also a low-complexity LEQ, although the number of operations is more than that of the MF-LEQ and that of the ZF-LEQ. This can be seen from Eq. (22), where the $(N+L)\times(N+L)$ inverse matrix is a fixed matrix, only required to be computed once. Therefore, $\boldsymbol{G}_{MMSE}$ is also fixed, with the dimensions of $N\times(N+L)$. In $\boldsymbol{G}_{MMSE}$ there will be more non-zero elements than in $\boldsymbol{G}_{MF}$ as well as in $\boldsymbol{G}_{ZF}$, and each column of $\boldsymbol{G}_{MMSE}$ has about $2L$ non-zero elements, if $N \geq 2L$. Hence, the number of operations required to compute $\tilde{\boldsymbol{z}} = \boldsymbol{G}\boldsymbol{y}$ is about $4L$. However, the benefit to employ the MMSE-LEQ is that it also has the capability to mitigate counting noise, which is useful in the case of high counting noise.

D. Decision Making

Having obtained the decision variable $\tilde{z}_u$, the uth bit can be detected relying on a threshold expressed as C_T. However, as the result of the ISI imposing on the current detection, we have to consider all the previously transmitted bits to compute the optimal threshold. For this objective, the receiver has to store all the estimated bits for current detection, and the estimation error would further decrease the error performance of the DMC system. In order to reduce the complexity of receiver and avoid the effect of error propagation from the previous detections, we consider the sub-optimal threshold based decision making. Specifically, when assuming that the binary information bits are uniformly distributed, we can approximately set $C_T = 0$ in decision making. In this case, the uth bit can be detected as

$$b_u = \begin{cases} 1, & \text{when } \tilde{z}_u > 0, \\ 0, & \text{when } \tilde{z}_u \leq 0. \end{cases} \tag{23}$$

Let us below provide some numerical results to demonstrate the performance of the equalizers considered in this section.

V. Performance Results and Analysis

In this section, we investigate and compare the bit error rate (BER) performance of the BMoSK-DMC systems employing different equalization schemes, as proposed in Sections IV. In our simulations, we assume that the coefficient of the two types of molecules diffusing in a liquid is $D = 2.2\times10^{-9}\ m^2/s$, the radius of receiver is set to $\rho = 15$ nm. As in [24], the SNR is defined as the ratio between the power received from a single pulse of molecules and the corresponding noise power generated by this molecular pulse, which is expressed as

$$\gamma_b = \frac{c_0^2}{E[\sigma_0^2]} = \frac{c_0^2}{\frac{1}{V}c_0} = Vc_0. \tag{24}$$

Hence, for a given SNR of γ_b, we can obtain $c_0 = \gamma_b/V = 3\gamma_b/(4\pi\rho^3)$. Applying this value and the associated values for $t = t_d$ and r into Eq. (1), we can obtain the number of molecules required to emit per pulse in simulations.

From the previous analysis we can know that the ISI length L is dependent on both the bit duration T_b and the transmission distance r. Correspondingly, in the following studies, L is estimated as

$$L \triangleq \arg_l\left\{c_l/c_0 \leq 1/1000\right\}. \tag{25}$$

In other words, the ISI from the samples having the concentration values at least 1000 times (30 dB) lower than c_0 of the pulse's peak value is ignored.

First, in Fig. 2, we compare the BER performance of the BMoSK-DMC systems employ the MF-LEQ, ZF-LEQ and MMSE-LEQ, respectively. In addition to the common parameters mentioned at the start of this section, the other parameters used in our simulation are provided with the figure and in the corresponding caption, the same are in the following figures. From Fig. 2, we can observe that for any LEQ scheme, the BER performance degrades as the transmission distance increases, which results in stronger ISI for a given bit rate of $1/T_b$. The results show that after suppressing the ISI,

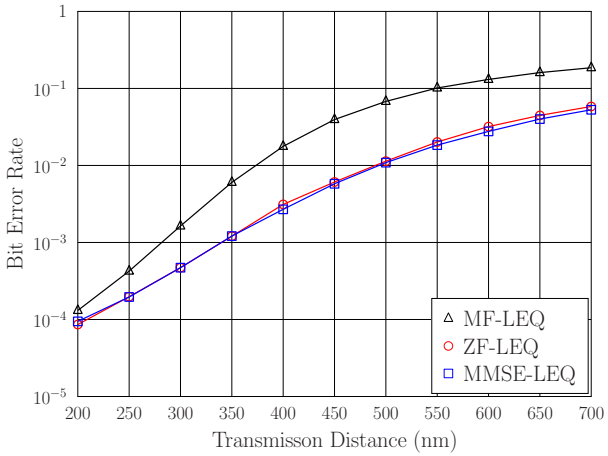

Fig. 2. Comparison of the BER performance of the BMoSK-DMC systems employing MF-LEQ, ZF-LEQ and MMSE-LEQ, when $N = 2L+1$, $\gamma_b = 12$ dB and $T_b = 5 \times 10^{-5}$ s.

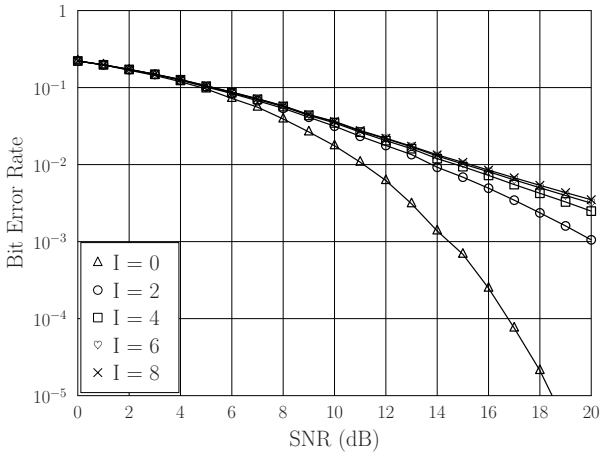

Fig. 3. BER performance of the different bits in the BMoSK-DMC systems with MF-LEQ, when $N = 2L + 1$, $r = 350nm$ and $T_b = 5 \times 10^{-5}$ s.

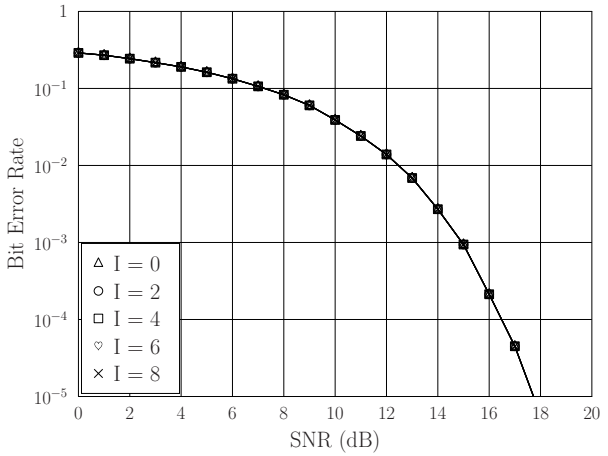

Fig. 4. BER performance of the different bits in the BMoSK-DMC systems with ZF-LEQ, when $N = 2L + 1$, $r = 650nm$ and $T_b = 8 \times 10^{-5}$ s.

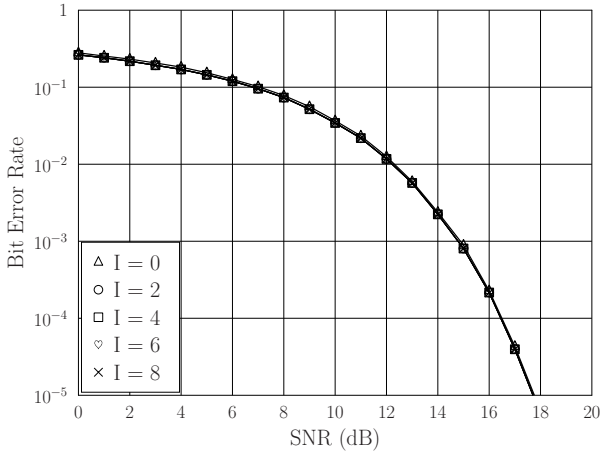

Fig. 5. BER performance of the different bits in the BMoSK-DMC systems with MMSE-LEQ, when $N = 2L + 1$, $r = 650nm$ and $T_b = 8 \times 10^{-5}$ s.

both the ZF-LEQ and MMSE-LEQ are capable of achieving much better performance than the MF-LEQ. Specifically, at the BER of 0.01, using the ZF-LEQ or MMSE-LEQ allows the BMoSK-DMC system to increase a transmission distance by about 125 nm, when compared with the MF-LEQ. Furthermore, Fig. 2 shows that both the ZF-LEQ and MMSE-LEQ achieve nearly the same performance, provided that the transmission distance is shorter than 500 nm. Beyond this distance, the MMSE-LEQ slightly outperforms the ZF-LEQ, owing to the MMSE-LEQ's noise suppression capability. Note that, as we mentioned previously in Section IV-B, in the BMoSK-DMC systems, the channel matrix $\boldsymbol{H}_d$ is a diagonal dominant matrix. Hence, the noise amplification problem of the ZF-LEQ operated in BMoSK-DMC systems is not severe. This can be explicitly evidenced by the results shown in Fig. 2, and also in the following figures.

In Figs. 3-5, we exam the BER of the bits at different locations of the detected blocks. Following Eq. (15), $I = 0$ represents the bit detected from $\tilde{z}_{N-1}$, $I = 1$ represents the bit detected from $\tilde{z}_{N-2}$, and so on. From Fig. 3 we can observe that when the value of I increases, the BER performance degrades. As what we analysed associated with Eq. (15), when I increases, the decision variable is able to collect more energy for detection, but also experiences higher interference. The results in Fig. 3 confirm that, when the MF-LEQ is employed, the added interference outweighs the extra energy collected from the ISI components, and hence dominates the final achievable performance. Therefore, in order to achieve the best possible performance by the MF-LEQ, we can simply form the decision variable as

$$\tilde{z}_u = c_0 z_u \triangleq z_u, \tag{26}$$

for detecting the uth bit, where z_u is given by Eq. (7). Here we have '$\triangleq$' due to c_0 being a positive constant. Note furthermore that the detector based on Eq. (26) is a symbol-based detector and has the lowest detection complexity.

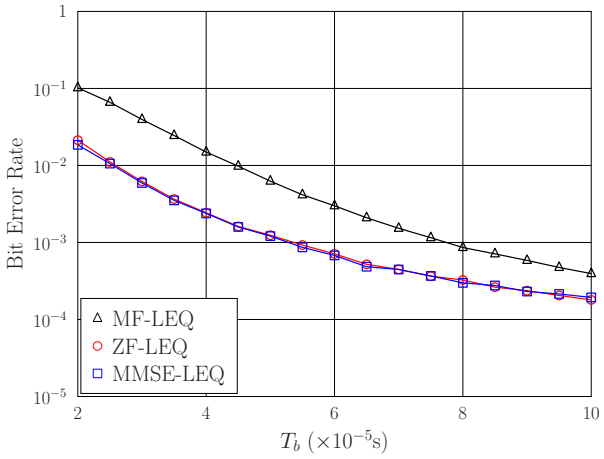

Fig. 6. Comparison of the BER versus bit duration T_b performance of the BMoSK-DMC systems employing MF-LEQ, ZF-LEQ and MMSE-LEQ, when $N = 2L + 1$, $r = 350$ nm and $\gamma_b = 12$ dB.

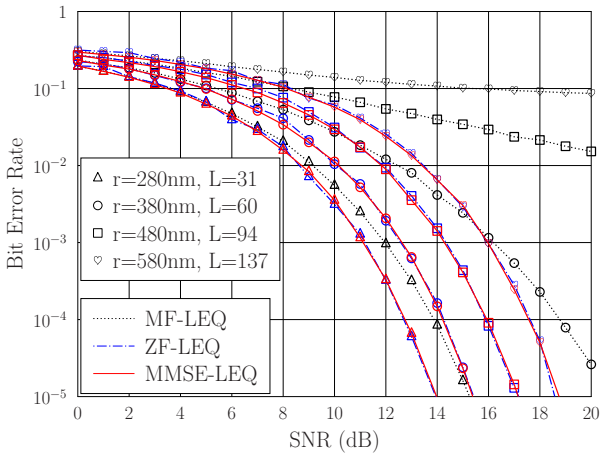

Fig. 7. Comparison of the BER performance of the BMoSK-DMC systems with MF-LEQ, ZF-LEQ and MMSE-LEQ, when $N = 2L+1$, $T_b = 5\times10^{-5}$ s.

By contrast, as shown in Figs. 4 and 5, after the ISI is suppressed by the ZF-LEQ or MMSE-LEQ, the detections of all the bits in one block achieve a similar BER performance, which is slightly better than that of MF-LEQ with $I = 0$.

In Fig.6, we show the effect of bit duration T_b (or bit rate $R_b = 1/T_b$ of the system) on the BER performance of the BMoSK-DMC systems employing the MF-LEQ, ZF-LEQ and MMSE-LEQ, respectively. Explicitly, as the bit rate decrease (or as the bit duration increases), the BER performance in all cases improves. This is because for a fixed transmission distance, the ISI reduces as the bit duration increases. Furthermore, both the ZF-LEQ and MMSE-LEQ achieve a similar BER performance, which outperform the MF-LEQ.

In the context of Fig.7, we investigate the impact of transmission distance on the BER performance of the BMoSK-DMC systems employing the MF-LEQ, ZF-LEQ and MMSE-LEQ, when a fixed bit duration is assumed. In this case, when the transmission distance becomes longer, the ISI length also increases, according to the properties of Eq. (1). The ISI length corresponding to different transmission distance is explicitly shown with the figure. Explicitly, due to the increase of the ISI resulted from the increase of transmission distance, for all the three LEQ schemes, the BER performance degrades as the transmission distance increases. From the results of Fig.7 we can be inferred that, provided that the SNR is sufficiently high, both the ZF-LEQ and MMSE-LEQ perform well, even when the transmission distance is as high as $r = 580$ nm. The BER performance achieved by the ZF-LEQ or MMSE-LEQ can significantly outperform that of the MF-LEQ, which becomes more declared, as the transmission distance becomes longer.

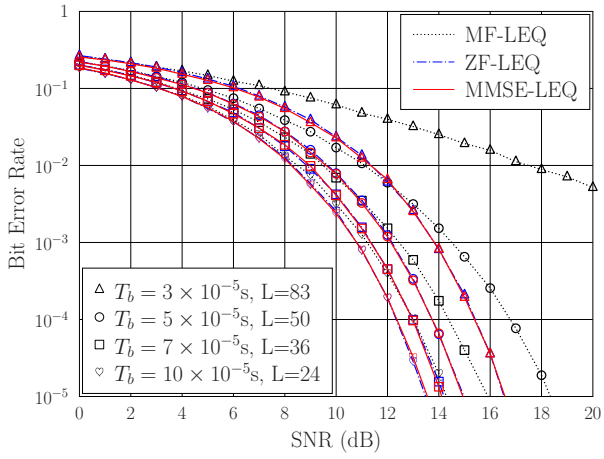

Fig. 8. Comparison of the BER performance of the BMoSK-DMC systems with MF-LEQ, ZF-LEQ and MMSE-LEQ, when $N = 2L + 1$ and $r = 350$ nm.

Finally in Fig.8, we demonstrate the impact of bit duration T_b on the BER performance of the BMoSK-DMC systems with MF-LEQ, ZF-LEQ and MMSE-LEQ, when a fixed transmission distance of $r = 350$ nm is assumed. In this case, when T_b is smaller, means that the bit rate is higher, the ISI becomes longer. Correspondingly, as seen in Fig.8, for all the three LEQ schemes, the BER performance improves, as T_b becomes larger or the bit rate becomes lower. Again, the BER performance attained by the ZF-LEQ or MMSE-LEQ outperforms that of the MF-LEQ, which is more significant, when ISI becomes stronger.

To this point, we would like to note that, regardless of which LEQ is employed, the BER performance of the BMoSK-DMC system at a given SNR degrades, whenever the ISI becomes stronger, no matter what the source is to make the ISI increase. This can be explicitly seen, e.g., in Figs. 6-8. This result is different from that in the conventional radio-based communication systems [37], where the advanced equalizers, including the ZF- and MMSE-based equalizers, are usually capable of achieving the performance of their corresponding systems without ISI. The reason behind is that in the conventional radio-based communication systems, the additive white

Gaussian noise (AWGN) is experienced, whose statistics have nothing to do with the transmitted signals. By contrast, in the DMC communication systems including the BMoSK-DMC system considered in this paper, as seen in Eq. (3)-Eq. (6), the noise components are related to the transmitted signals. It can be known that even when uniformly distributed data bits are assumed, the second moment of the noise components, i.e., the noise power, increases with the increase of ISI. Due to this increase of noise power, we can know that for a SNR given by Eq. (24), the actual SNR determining the achievable performance in fact decreases with the increase of ISI. Hence, the resultant BER performance always degrades, as the ISI becomes stronger.

VI. Conclusion

In this paper, we have investigated the receiving equalization techniques for the ISI mitigation and signal detection in BMoSK-DMC systems. Three types of LEQs have been considered, namely the MF-LEQ, ZF-LEQ and MMSE-LEQ. We have examined the effects of the different parameters defining transmit signals and characterizing DMC channels on the error performance of the BMoSK-DMC systems. Our studies and performance results show that to achieve the best possible performance, the MF-LEQ is reduced to a symbol-based detector, which detects individual bits independently under the ISI. In BMoSK-DMC systems, the channel matrix is diagonal dominant, which makes the ZF-LEQ highly efficient, achieving nearly the same performance as the MMSE-LEQ, although MMSE-LEQ has a slightly higher complexity than the ZF-LEQ. Both the ZF-LEQ and MMSE-LEQ are capable of effectively suppressing the ISI, yielding significantly improved detection reliability beyond the MF-LEQ. Nevertheless, both the ZF-LEQ and MMSE-LEQ are still low-complexity equalizers that are feasible for implementation, although their complexity is slightly higher than that of the MF-LEQ.

References

[1] Farsad, N., Yilmaz, H.B., Eckford, A., Chae, C.B., Guo, W.: 'A comprehensive survey of recent advancements in molecular communication', *IEEE Communications Surveys Tutorials*, 2016, **18**, (3), pp. 1887–1919

[2] Nakano, T., Suda, T., Okaie, Y., Moore, M.J., Vasilakos, A.V.: 'Molecular communication among biological nanomachines: A layered architecture and research issues', *IEEE Transactions on NanoBioscience*, 2014, **13**, (3), pp. 169–197

[3] Unluturk, B.D., Akyildiz, I.F.: 'An end-to-end model of plant pheromone channel for long range molecular communication', *IEEE Transactions on NanoBioscience*, 2017, **16**, (1), pp. 11–20

[4] Chude.Okonkwo, U.A.K., Malekian, R., Maharaj, B.T.S.: 'Molecular communication model for targeted drug delivery in multiple disease sites with diversely expressed enzymes', *IEEE Transactions on NanoBioscience*, 2016, **15**, (3), pp. 230–245

[5] Aghababaiyan, K., Shah-Mansouri, V., Maham, B. 'Capacity bounds of neuro-spike communication by exploiting temporal modulations'. In: 2018 IEEE Wireless Communications and Networking Conference (WCNC). 2018. pp. 1–6

[6] Aghababaiyan, K., Maham, B. 'Error probability analysis of neuro-spike communication channel'. In: 2017 IEEE Symposium on Computers and Communications (ISCC). 2017. pp. 932–937

[7] Aghababaiyan, K., Shah-Mansouri, V., Maham, B. 'Asynchronous neuro-spike array - based communication'. In: 2018 IEEE International Black Sea Conference on Communications and Networking (BlackSeaCom). 2018. pp. 1–5

[8] Ankit, Bhatnagar, M.R.: 'Boolean AND and OR logic for cell signalling gateways: a communication perspective', *IET Nanobiotechnology*, 2018, **12**, (8), pp. 1130–1139

[9] Kuran, M.S., Tugcu, T., Edis, B.O.: 'Calcium signaling: overview and research directions of a molecular communication paradigm', *IEEE Wireless Communications*, 2012, **19**, (5), pp. 20–27

[10] Nakano, T., Okaie, Y., Kobayashi, S., Hara, T., Hiraoka, Y., Haraguchi, T.: 'Methods and applications of mobile molecular communication', *Proceedings of the IEEE*, 2019, **107**, (7), pp. 1442–1456

[11] Grebenstein, L., Kirchner, J., Peixoto, R.S., Zimmermann, W., Irnstorfer, F., Wicke, W., et al.: 'Biological optical-to-chemical signal conversion interface: A small-scale modulator for molecular communications', *IEEE Transactions on NanoBioscience*, 2019, **18**, (1), pp. 31–42

[12] Feng, L., Ali, A., Iqbal, M., Bashir, A.K., Hussain, S.A., Pack, S.: 'Optimal haptic communications over nanonetworks for E-health systems', *IEEE Transactions on Industrial Informatics*, 2019, **15**, (5), pp. 3016–3027

[13] Salehi, S., Moayedian, N.S., Haghjooy Javanmard, S., Alarcon, E.: 'Lifetime improvement of a multiple transmitter local drug delivery system based on diffusive molecular communication', *IEEE Transactions on NanoBioscience*, 2018, **17**, (3), pp. 352–360

[14] Aghababaiyan, K., Shah-Mansouri, V., Maham, B.: 'Axonal channel capacity in neuro-spike communication', *IEEE Transactions on NanoBioscience*, 2018, **17**, (1), pp. 78–87

[15] Aghababaiyan, K., Shah-Mansouri, V., Maham, B.: 'Joint optimization of input spike rate and receiver decision threshold to maximize achievable bit rate of neuro-spike communication channel', *IEEE Transactions on NanoBioscience*, 2019, **18**, (2), pp. 117–127

[16] Nakano, T., Liu, J.Q.: 'Design and analysis of molecular relay channels: An information theoretic approach', *IEEE Transactions on NanoBioscience*, 2010, **9**, (3), pp. 213–221

[17] Pierobon, M., Akyildiz, I.F.: 'Diffusion-based noise analysis for molecular communication in nanonetworks', *IEEE Transactions on Signal Processing*, 2011, **59**, (6), pp. 2532–2547

[18] Aghababaiyan, K., Zefreh, R.G., Shah-Mansouri, V.: 'Enhancing data rate of molecular communication system using Brownian motion', *IET Nanobiotechnology*, 2019, **13**, (3), pp. 293–300

[19] Kuran, M.S., Yilmaz, H.B., Tugcu, T., Akyildiz, I.F. 'Modulation techniques for communication via diffusion in nanonetworks'. In: 2011 IEEE International Conference on Communications (ICC). 2011. pp. 1–5

[20] Eckford, A.W. 'Achievable information rates for molecular communication with distinct molecules'. In: Bio-Inspired Models of Network, Information and Computing Systems, 2007. Bionetics 2007. 2nd. 2007. pp. 313–315

[21] Tepekule, B., Pusane, A.E., Yilmaz, H.B., Chae, C., Tugcu, T.: 'ISI mitigation techniques in molecular communication', *IEEE Transactions on Molecular, Biological and Multi-Scale Communications*, 2015, **1**, (2), pp. 202–216

[22] Arjmandi, H., Movahednasab, M., Gohari, A., Mirmohseni, M., Nasiri-Kenari, M., Fekri, F.: 'ISI-avoiding modulation for diffusion-based molecular communication', *IEEE Transactions on Molecular, Biological and Multi-Scale Communications*, 2017, **3**, (1), pp. 48–59

[23] Shi, L., Yang, L.L. 'Diffusion-based molecular communications: Inter-symbol interference cancellation and system performance'. In: 2016 IEEE/CIC International Conference on Communications in China (ICCC). 2016. pp. 1–6

[24] Shi, L., Yang, L.: 'Error performance analysis of diffusive molecular communication systems with on-off keying modulation', *IEEE Transactions on Molecular, Biological and Multi-Scale Communications*, 2017, **3**, (4), pp. 224–238

[25] Meng, L.S., Yeh, P.C., Chen, K.C., Akyildiz, I.F.: 'On receiver design for diffusion-based molecular communication', *IEEE Transactions on Signal Processing*, 2014, **62**, (22), pp. 6032–6044

[26] Tepekule, B., Pusane, A.E., Kuran, M.A., Tugcu, T.: 'A novel pre-equalization method for molecular communication via diffusion in nanonetworks', *IEEE Communications Letters*, 2015, **19**, (8), pp. 1311–1314

[27] Li, B., Sun, M., Wang*, S., Guo, W., Zhao, C.: 'Low-complexity noncoherent signal detection for nanoscale molecular communications', *IEEE Transactions on NanoBioscience*, 2016, **15**, (1), pp. 3–10

[28] Li, B., Sun, M., Wang, S., Guo, W., Zhao, C.: 'Local convexity inspired low-complexity noncoherent signal detector for nanoscale molecular communications', *IEEE Transactions on Communications*, 2016, **64**, (5), pp. 2079–2091

[29] Akdeniz, B.C., Pusane, A.E., Tugcu, T.: 'Optimal reception delay in diffusion-based molecular communication', *IEEE Communications Letters*, 2018, **22**, (1), pp. 57–60

[30] ShahMohammadian, H., G..Messier, G., Magierowski, S.: 'Optimum receiver for molecule shift keying modulation in diffusion-based molecular communication channels', *Nano Communication Networks*, 2012, **3**, pp. 183-195

[31] Kilinc, D., Akan, O.B.: 'Receiver design for molecular communication', *IEEE Journal on Selected Areas in Communications*, 2013, **31**, (12), pp. 705–714

[32] Noel, A., Cheung, K.C., Schober, R.: 'Optimal receiver design for diffusive molecular communication with flow and additive noise', *IEEE Transactions on NanoBioscience*, 2014, **13**, (3), pp. 350–362

[33] Chou, C.T.: 'A markovian approach to the optimal demodulation of diffusion-based molecular communication networks', *IEEE Transactions on Communications*, 2015, **63**, (10), pp. 3728–3743

[34] Koo, B., Yilmaz, H.B., Eckford, A.W., Chae, C.B.: 'Detection algorithms for molecular mimo', *2015 IEEE International Conference on Communications (ICC)*, 2015, pp. 1122–1127

[35] Koo, B.H., Lee, C., Yilmaz, H.B., Farsad, N., Eckford, A., Chae, C.B.: 'Molecular MIMO: From theory to prototype', *IEEE Journal on Selected Areas in Communications*, 2016, **34**, (3), pp. 600–614

[36] Mosayebi, R., Arjmandi, H., Gohari, A., Nasiri.Kenari, M., Mitra, U.: 'Receivers for diffusion-based molecular communication: Exploiting memory and sampling rate', *IEEE Journal on Selected Areas in Communications*, 2014, **32**, (12), pp. 2368–2380

[37] Proakis, J.G.: 'Digital Communications'. 5th ed. (McGraw Hill, 2007)

[38] Yang, L.L.: 'Multicarrier Communications'. (Wiley, 2009)